Version 1.0
October, 2002

Cosmic Origins Spectrograph Instrument Mini-Handbook for Cycle 12

Available in Cycle 13
Do not propose for COS in Cycle 12

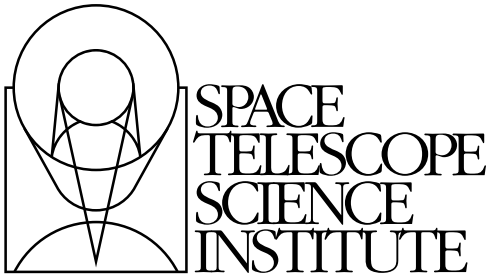

Space Telescope Science Institute
3700 San Martin Drive
Baltimore, Maryland 21218
help@stsci.edu

Operated by the Association of Universities for Research in Astronomy, Inc., for the National Aeronautics and Space Administration

User Support

For prompt answers to any question, please contact the STScI Help Desk.

- **E-mail:** help@stsci.edu
- **Phone:** (410) 338-1082
  (800) 544-8125 (U.S., toll free)

World Wide Web

Information and other resources are available on the COS World Wide Web site:

- **URL:** http://www.stsci.edu/instruments/cos

COS History

Version	Date	Editor
1.0	October 2002	Kenneth Sembach

Contributors:

Kenneth Sembach, Charles Keyes, Claus Leitherer, Jon Morse, Steven Penton, Erik Wilkinson.

Citation:

In publications, refer to this document as:
Sembach, K.R. et al. 2002, in Cosmic Origins Spectrograph Instrument Mini-Handbook, version 1.0, (Baltimore, STScI)

Send comments or corrections to:
Space Telescope Science Institute
3700 San Martin Drive
Baltimore, Maryland 21218
E-mail:help@stsci.edu

Table of Contents

Preface

This document describes the observing capabilities that are to be offered by the Cosmic Origins Spectrograph (COS) on the Hubble Space Telescope (HST) in the next Call for Proposals (Cycle 13). COS is not available for use during the current proposal cycle (Cycle 12). This document provides a brief preview of the COS instrument capabilities and comparisons with the capabilities of earlier generation instruments, such as the Space Telescope Imaging Spectrograph (STIS).

A more complete Instrument Handbook for COS will be provided as part of the Cycle13 Call for Proposals. The sensitivities and specifications outlined in the present document should be treated as provisional since COS had not yet completed ground testing at the time this handbook was written.

Cosmic Origins Spectrograph

In this book. . .

1. Overview

The Cosmic Origins Spectrograph (COS) is a fourth-generation instrument to be installed on the Hubble Space Telescope (HST) during the 2004 servicing mission[1]. COS is designed to perform high sensitivity, moderate- and low-resolution spectroscopy of astronomical objects in the 1150–3200 Å wavelength range. COS will significantly enhance the spectroscopic capabilities of HST at ultraviolet wavelengths, and will provide observers with unparalleled opportunities for observing faint sources of ultraviolet light. COS is not meant to be a replacement for the Space Telescope Imaging Spectrograph (STIS), which will remain in HST after the servicing mission and will be available to the community. Each instrument has unique capabilities, which we compare and summarize in this document.

1. COS will be inserted into the HST bay currently housing COSTAR, the Corrective Optics Space Telescope Axial Replacement, which is no longer needed to correct for the spherical aberration in the HST primary mirror.

1.1 Instrument Overview

COS has a simple optical design that minimizes the number of reflections required to disperse and detect ultraviolet light in its two optical channels. The instrument is optimized for high-throughput spectroscopy of point sources but may also be used to observe extended objects, albeit with limited spatial information and degraded spectral resolution.

Light enters COS through a 2.5 arcsec diameter circular aperture and encounters an optical element that enables far-ultraviolet (FUV; $1150 < \lambda <$ 2050 Å) or near-ultraviolet (NUV; $1700 < \lambda < 3200$ Å) observations. In the FUV channel, the light illuminates a single optical element – a concave holographically-ruled diffraction grating. An optic selection mechanism configures either the low-dispersion grating or one of two medium-dispersion gratings for the observation. The grating disperses the light, corrects for the HST spherical aberration, and focuses the light onto a crossed delay-line microchannel plate (MCP) detector. The same selection mechanism may also be used to place a mirror in the light path in place of the grating for NUV observations. The COS FUV optical path is illustrated schematically in Figure 1.

Figure 1: The COS FUV optical path. Only one reflection is required to place the dispersed light onto the FUV microchannel plate detector. An optic selection mechanism configures one of the gratings for the observation. A mirror can also be inserted in place of the FUV grating to divert light into the COS NUV channel.

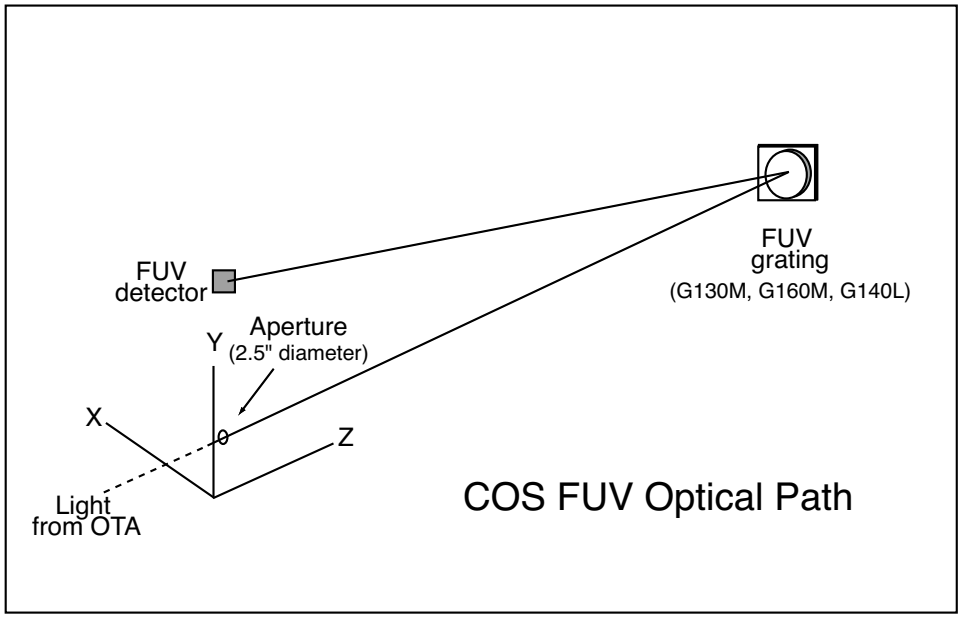

Figure 2: The COS NUV optical path. Four reflections are required to place the light onto the NUV MAMA detector. The NCM1 mirror is placed in the light path by the FUV optical element selection mechanism.

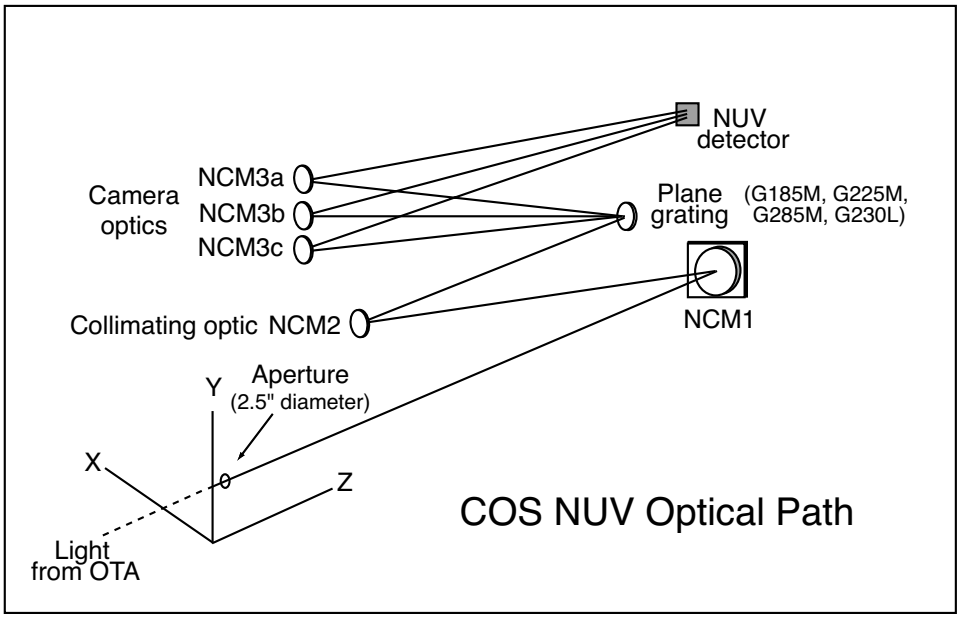

Light entering the NUV channel encounters four optical elements (3 mirrors and a holographically-ruled plane diffraction grating) before reaching a multi-anode microchannel array (MAMA) detector. The larger number of reflections reduces the throughput of this channel compared to the FUV channel, but allows for a compact Czerny-Turner design. The COS NUV optical path is illustrated schematically in Figure 2. A second optic selection mechanism specific to this channel configures either a low-dispersion grating or one of three medium-dispersion plane gratings for spectroscopic observations. An additional optical element, a target acquisition mirror, can be placed in the light path in place of the grating to obtain target confirmation images or perform imaging target acquisitions.

1.2 STScI Contact Information

Table 1 lists the COS Instrument Division contacts at STScI. Observers seeking more detailed information about the COS instrument performance or operations should contact one of the COS instrument scientists. Observers may also direct questions to the Help Desk at STScI. To contact the Help Desk,

- Send E-mail to: help@stsci.edu
- Phone: 410-338-1082

Table 1: COS Instrument Division Contacts at STScI

Contact Person	E-mail	Phone	Responsibility
Charles (Tony) Keyes	keyes@stsci.edu	410-338-4975	Instrument Scientist
Kenneth Sembach	sembach@stsci.edu	410-338-5051	Instrument Scientist
Claus Leitherer	leitherer@stsci.edu	410-338-4425	Instrument Scientist
Scott Friedman	friedman@stsci.edu	410-338-4906	Instrument Scientist

1.3 The COS Instrument Definition Team

The COS Instrument Definition Team (IDT) is responsible for the development, management, and scientific oversight of COS prior to launch. The COS IDT has approximately 550 orbits of guaranteed observing time with the instrument. The IDT observing time will occur primarily in Cycle 13, with a portion of the time remaining for observations in Cycles 14 and 15. Key personnel on the COS IDT include:

- ***Principal Investigator***: James Green (University of Colorado)
- ***Project Scientist***: Jon Morse (University of Colorado)
- ***Instrument Scientist***: Erik Wilkinson (University of Colorado)
- ***Experiment Manager***: John Andrews (University of Colorado)
- ***Co-Investigators***: Dennis Ebbets (Ball Aerospace), Sara R. Heap (GSFC), Claus Leitherer (STScI), Jeffrey Linsky (U. Colorado), Blair D. Savage (U. Wisconsin), J. Michael Shull (U. Colorado), Oswald Siegmund (U. California-Berkeley), Theodore P. Snow (U. Colorado), S. Alan Stern (Southwest Research Institute), and John T. Stocke (U. Colorado).
- ***Primary Contractor***: Ball Aerospace

1.4 Handbook Information and Additional Resources

Resources used in the preparation of this document include COS OP-01 (Morse et al. 2002, Rev. 17 and references therein) and the STIS Instrument Handbook (Leitherer et al. 2001, v5.1). We thank the COS IDT members for their assistance with the preparation of this document, particularly Erik Wilkinson, Jon Morse, and Steven Penton. Additional COS information and planning tools, including a link to a preliminary spectral simulator, can be found on the COS webpage at http://www.stsci.edu/instruments/cos/.

2. Instrument Description

2.1 Detectors

The two COS detectors are photon-counting devices that convert light focused on their photosensitive front surfaces into streams of digitized photon coordinates. Basic information about each detector is provided in Table 2.

Table 2: COS Detectors

		FUV MCP	NUV MAMA
Photocathode		CsI (opaque)	Cs_2Te (semi-transparent)
Window		None	MgF_2 (re-entrant)
Wavelength range		1150 – 2050 Å	1700 – 3200 Å
Active area		85 x 10 mm (two)	25.6 x 25.6 mm
Pixel format		16384 x 1024 (two)	1024 x 1024
Pixel size		6 x 24 μm	25 x 25 μm
Spectral resolution element size		6 x 10 pix	3 x 3 pix
Quantum efficiency		26% at 1335 Å 12% at 1560 Å	10% at 2200 Å 8% at 2800 Å
Dark count rate		~0.5 cnt s^{-1} cm^{-2} ~$7.2x10^{-7}$ cnt s^{-1} pix^{-1} ~$4.3x10^{-5}$ cnt s^{-1} $resel^{-1}$	~34 cnt s^{-1} cm^{-2} ~$2.1x10^{-4}$ cnt s^{-1} pix^{-1} ~$1.9x10^{-3}$ cnt s^{-1} $resel^{-1}$
Detector global count rate limit	TTAG	~21,000 cnt s^{-1}	~21,000 cnt s^{-1}
	ACCUM	~60,000 cnt s^{-1} $segment^{-1}$	~170,000 cnt s^{-1}
Local count rate limit		~100 cnt s^{-1} $resel^{-1}$ ~1.67 cnt s^{-1} pix^{-1}	~1800 cnt s^{-1} $resel^{-1}$ ~200 cnt s^{-1} pix^{-1}

Note: Global and local count rate limits are approximate values set by a combination of hardware, flight software, and memory management considerations. Descriptions of the count rate limits for all operational modes will be given in the COS Instrument Handbook.

The FUV detector is a windowless, crossed delay-line MCP stack optimized for the 1150 to 1775 Å bandpass. The active front surface of the detector is curved to match the focal surface radius of curvature of 826 mm. To achieve the length required to capture the entire projected COS spectrum, two detector segments are placed end to end with a small gap between them. The two detector segments are independently operable; loss of one segment does not compromise the independent operation of the

other. Each detector segment has an active area of 85 x 10 mm digitized to 16384 x 1024 pixels.

The NUV detector is a multi-anode microchannel array (MAMA) optimized for spectroscopic observations in the 1700–3200 Å bandpass. Target acquisitions that are not performed with dispersed light in the FUV channel are performed in the NUV channel with this detector. The COS MAMA is similar to the NUV MAMA used on STIS – the COS detector is the backup for the STIS NUV MAMA flight unit. The MAMA high-resolution (pixel sub-sampling) mode available with STIS will not be supported for COS.

2.2 Spectroscopic Modes

COS supports medium-resolution ($R = \lambda/\Delta\lambda \sim 16{,}000–24{,}000$) and low-resolution ($R \sim 2000–3000$) spectroscopic observations in both the FUV and NUV channels. Observations cannot be obtained simultaneously in both channels. A summary of the available spectroscopic modes is provided in Table 3.

All of the dispersive elements are holographically-ruled, ion-etched diffraction gratings with excellent scattered light properties and reflectivities. The gratings have Al+MgF2 coatings, except the G225M and G285M gratings, which have bare Al coatings.

Table 3: COS Spectroscopic Modes

Optical Element	λ Range (Å)	λ Coverage (Å per tilt)	Resolving Power (λ/Δλ)	Dispersion (Å/pix)
FUV MCP Detector				
G130M	1150 –1450	300	20,000 – 24,000	~0.0094
G160M	1405 – 1775	370	20,000 – 24,000	~0.0118
G140L	1230 – 2050	>820	2500 – 3000	~0.0865
NUV MAMA Detector				
G185M	1700 – 2100	3 x 35	16,000 – 20,000	~0.0342
G225M	2100 – 2500	3 x 35	20,000 – 24,000	~0.0342
G285M	2500 – 3000	3 x 41	20,000 – 24,000	~0.0400
G230L	1700 – 3200	(1 or 2) x 398	1550 – 2900	~0.3887

For spectroscopic observations in the FUV channel, light illuminating the COS entrance aperture falls directly on the selected grating, where it is dispersed and focused onto the FUV detector. The FUV spectra fall on a continuous strip of the detector, with a small gap between the two detector

segments. In the medium dispersion modes (G130M, G160M), this gap has a width of about 20 Å. The gratings can be rotated slightly to allow gap coverage. In the low-dispersion mode (G140L), the gap is larger (~135 Å) and can be used to mask out the Lyα geocoronal emission with an appropriate choice of grating tilt.

For spectroscopic observations in the NUV channel, light illuminating the entrance aperture is reflected by a mirror, which corrects for the HST spherical aberration, magnifies the beam by a factor of four, and directs the light to a collimating optic. The collimating optic reflects the light to one of several flat first-order diffraction gratings, which disperse the light and reflect the beam to three camera optics, which image the light onto the detector. In the medium-resolution modes, the NUV spectra appear as three non-contiguous 35–41 Å stripes on the detector (~105–123 Å total coverage per exposure). A series of exposures at different central wavelengths will be needed to cover the entire NUV wavelength range. In the low-resolution mode, one or two 398 Å stripes will be present, and a total of three exposures will be needed to cover the entire wavelength range.

Table 4: Selected STIS Spectroscopic Modes

Optical Element	λ Range (Å)	λ Coverage (Å per tilt)	Resolving Power (λ/Δλ)	Dispersion (Å/pix)
FUV MAMA Detector				
E140H	1140 –1700	210	110,000	λ/228,000
E140M	1123 – 1710	620	45,800	λ/91,700
G140M	1140 – 1740	55	10,000	0.05
G140L	1150 – 1730	610	1000	0.6
NUV MAMA Detector				
E230H	1620 – 3150	267	110,000	λ/228,000
E230M	1570 – 3110	800	30,000	λ/60,000
G230M	1640 – 3100	90	10,000	~0.09
G230L	1570 – 3180	1610	500	~1.58
NUV CCD Detector				
G230MB	1640 – 3190	155	6,000	~0.15
G230LB	1680 – 3060	1380	700	~1.35

Note: Additional STIS modes are available, but those listed above are the most common modes for point source spectroscopy – see the STIS Instrument Handbook for more details.

The parameters for a selected set of spectroscopic modes available with STIS are summarized in Table 4 for comparison with the COS spectroscopic modes in Table 3. These are the most commonly used STIS modes for point source observations. A variety of apertures and additional modes (not listed) are available for spectroscopic and imaging observations of extended sources. Note that COS and STIS define resolving power slightly differently because the COS spectral line spread function (LSF) is fully sampled by the detector, while the STIS LSF is nearly fully sampled. For the purposes of the comparison, the value of $\Delta\lambda$ assumed for COS is the FWHM of the LSF, while the value of $\Delta\lambda$ assumed for STIS is equivalent to twice the dispersion per pixel (i.e., a Nyquist sampling frequency of 2 pixels for the FWHM is assumed).

2.3 Apertures

COS has two circular science apertures that are 2.5 arcsec in diameter. The primary science aperture (PSA) is a full-transmission aperture expected to be used for most normal science observations. This aperture transmits all of the light from a well-centered, aberrated point source image delivered by the HST optical telescope assembly (OTA). The bright object aperture (BOA) is used for observations requiring flux attenuation. The BOA contains a neutral density (ND2) filter that attenuates the flux by a factor of 100 (5 magnitudes). Both apertures will be fully calibrated and available for use.

The COS science apertures are field stops and are not traditional entrance slits like those used on STIS and earlier HST spectrographs. Thus, they do not project sharp edges on the detectors. Because COS is a slitless spectrograph, the spectral resolution depends on the nature of the astronomical object being observed. Though not optimized for observations of extended objects, COS can be used to detect faint diffuse sources with lower spectral resolution than would be achieved for point (< 0.1 arcsec) sources.

2.4 Photon Event Counting and Spectrum Accumulation

COS exposures on each detector may be obtained in either a time-tagged photon address (TTAG) mode, in which the position and time of each detected photon are saved in an event stream, or in accumulation (ACCUM) mode in which the positions, but not the times, of the photon events are recorded. The TTAG mode of recording events allows the post-observation pipeline processing system to screen the data as a function of time, if desired. The COS TTAG mode has a time resolution of 32 ms.

Pulse height information is available for all COS FUV science exposures. No pulse height information is available for COS NUV science

exposures. The pulse height distribution (PHD) is an important diagnostic of the quality of any spectrum obtained with microchannel plate detectors. Pulse height screening is useful for reducing unwanted background events, and can often improve the signal-to-noise ratio in the extracted science spectrum. In ACCUM mode, the global PHD is accumulated on-board as a separate data product along with the photon events. In TTAG mode, the individual pulse height amplitudes are recorded along with the position and time information of the photon events, so the PHD can be screened by time or position on the detector if desired.

2.5 Calibration Observations

Most COS calibration observations will be obtained as part of Observatory on-orbit calibration activities. These will include flux calibration observations of photometric standard stars, Pt-Ne wavelength calibration spectra, flatfields, and dark (background) level monitoring. Wavelength calibration exposures will be obtained automatically whenever a grating is selected. Observers will also be able to specify additional wavelength calibration exposures if desired. The COS specifications for absolute and relative wavelength determinations within an exposure are ±15 km s^{-1} and ±5 km s^{-1}, respectively; it may be possible to obtain information that could improve this performance. Internal flatfields and darks will be restricted to Observatory calibration programs only.

2.6 Signal-to-Noise Considerations

COS will be capable of routinely delivering fully reduced spectra with a signal-to-noise (S/N) ratio of ~20-30 per resolution element in single exposures at specific grating settings. Higher S/N ratios may be attainable, depending on the quality of the flatfield images obtained as part of the instrument calibration program. In addition, COS science exposures can be obtained at slightly different focal plane positions in the dispersion direction. Alignment and co-addition of these "FP-split" sub-exposures may further reduce the effects of fixed-pattern noise in the final calibrated spectrum and may allow for substantial increases in the S/N ratio. A quantitative assessment of the fixed-pattern noise present in COS spectra and its reduction in the calibration process will be made during ground testing of the instrument.

2.7 Observing Extended Sources

COS is capable of observing extended sources, but the amount of spatial information is limited. COS can distinguish between two point sources with a separation of ~1 arcsec in the cross-dispersion direction. Thus, for

an extended source, there are roughly two spatial resolution elements covered by the science aperture, but these spatial elements are not completely independent since the astigmatism of the optics blends the light. Unlike STIS, where a slit that is imaged by the optics can be used to isolate a portion of the source and preserve spectral resolution, the COS apertures are of a single size and receive an aberrated beam. Observations of extended sources will have a spectral resolution that is degraded compared to that of a point source. An observation of an object with an extent of ~0.5 arcsec will have a resolving power of $\lambda/\Delta\lambda \sim 5000$ with the medium-resolution gratings. An observation of an object that uniformly illuminates the aperture will have a resolving power of only $\lambda/\Delta\lambda \sim 1500$–$2000$ with the medium-resolution gratings.

3. Throughputs and Sensitivities

3.1 Throughputs and Effective Areas

Detailed measurements of the throughputs of the COS optical systems have not yet been made during ground testing of the instrumentation. Component testing indicates that COS should be considerably more sensitive than STIS and earlier generation HST instruments at comparable spectral resolutions. Preliminary results for the end-to-end system throughputs of the COS FUV and NUV channels are shown in Figures 3 and 4. These estimates are appropriate for a point source centered in the COS primary science aperture. The throughput and effective area calculations include the throughput of the HST OTA and degradation of the light beam prior to entry into the COS instrumentation, as described by Burrows (1988, STScI internal memo). At FUV wavelengths, the peak effective area is expected to reach ~2700 cm^2 near 1300 Å with the G130M grating. At NUV wavelengths, the peak effective area is expected to reach ~1000 cm^2 near 2350 Å with the G225M grating.

For comparison, similar calculations for several STIS MAMA spectroscopic modes covering the same ultraviolet wavelengths are also shown in Figures 3 and 4. At FUV wavelengths the system throughput with the COS medium-resolution mode is at least a factor of 7 higher than for the STIS medium-resolution echelle mode (E140M) and is a factor of ~2 or more higher than for the STIS low-resolution mode (G140L), neglecting STIS slit transmission losses (which are typically 30% or more). At NUV wavelengths, the COS medium-resolution throughput is at least a factor of 2 higher than it is for the STIS medium-resolution echelle mode (E230M) and exceeds the throughput of the STIS low-resolution mode (G230L) at $\lambda < 2200$ Å.

Figure 3: HST/COS FUV effective areas and throughputs. Values for several STIS modes are also shown for comparison with the COS values. All values are system end-to-end values that include the performance of the HST OTA, as described by Burrows (1988). All STIS values shown assume full slit transmission.

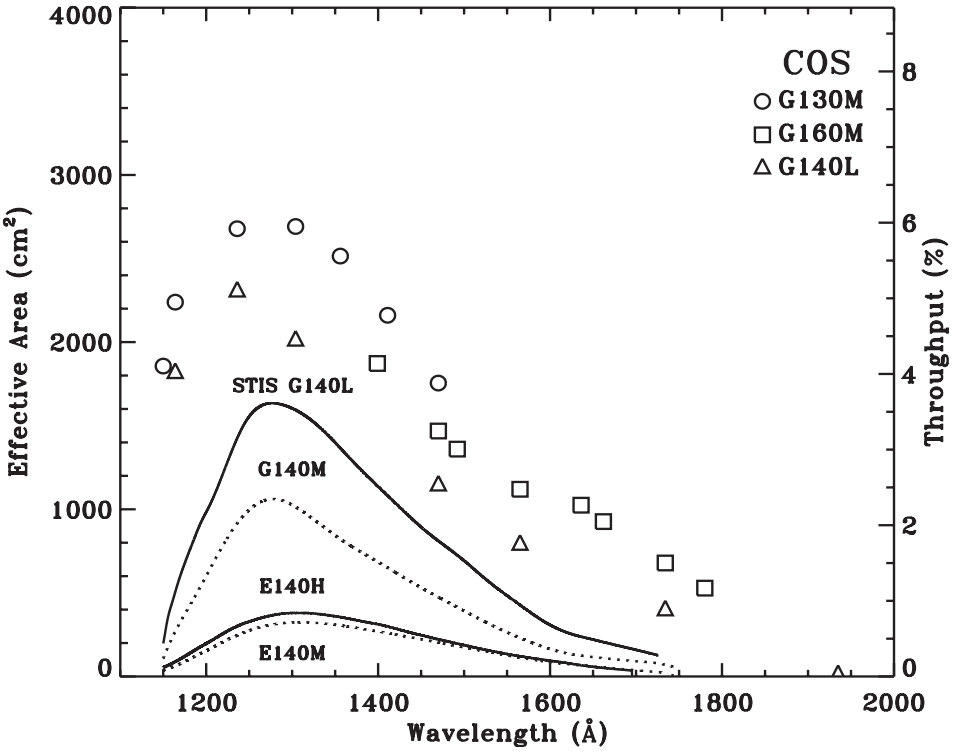

Figure 4: HST/COS NUV effective areas and throughputs. Values for several STIS modes are also shown for comparison with the COS values. All values are system end-to-end values that include the performance of the HST OTA, as described by Burrows (1988). All STIS values shown assume full slit transmission.

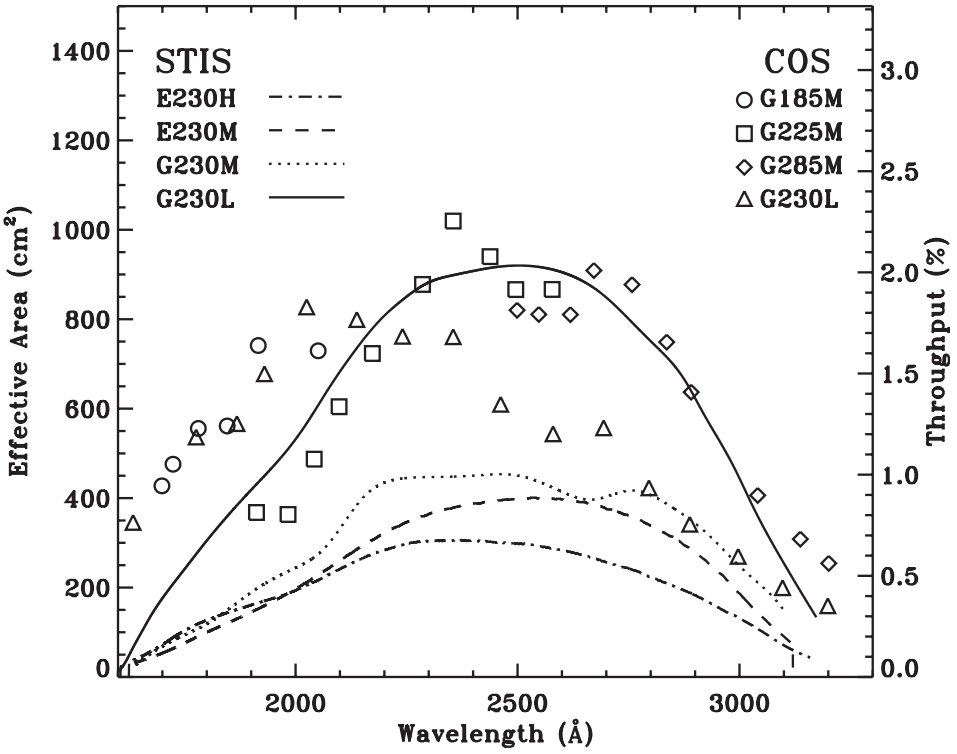

For clarity, we have not shown the STIS G230MB and G230LB throughput curves in Figure 4. At $\lambda > 2400$ Å, the STIS G230LB throughput exceeds 2.3%, and at $\lambda > 2800$ Å the STIS G230MB throughput exceeds 2.2%. Thus, for some programs that require high sensitivity at longer wavelengths, observations with these two lower resolution gratings and the STIS CCD may be suitable alternatives to observations with COS.

3.2 Point Source Sensitivities

Figures 5 and 6 show the point source sensitivities (S_λ) for the COS spectroscopic modes in units of counts per second per resolution element per incident erg cm^{-2} s^{-1} $Å^{-1}$. An estimate of the number of counts (N) expected per resolution element in an amount of time (Δt) for a source flux (F_λ) is given by $N = F_\lambda S_\lambda \Delta t$. As an example, with the COS G130M grating at 1300 Å an exposure time of approximately 9200 seconds is required to reach S/N = 30 per 0.065Å resolution element (R ~ 20,000) for an object with $F_{1300} \sim 1x10^{-14}$ erg cm^{-2} s^{-1} $Å^{-1}$. The same exposure with the STIS E140M mode and the 0.2"x0.2" aperture (binned by a factor of 2.3 to a resolution R~ 20,000) would take approximately $1.7x10^5$ seconds after accounting for the STIS scattered-light backgrounds and slit losses. All COS sensitivity estimates shown in Figures 5 and 6 are estimates only at this time since the instrument has not undergone full ground testing and calibration.

Table 5 compares the COS sensitivities to those of various STIS spectroscopic modes. The sensitivity depends upon the size of the spectral resolution element. Thus, for each mode, values for both the native resolution and binned resolution of the mode are provided to make these comparisons easier.

3.3 Bright Limits

Microchannel plates are susceptible to degradation if exposed to bright sources of ultraviolet light. Like STIS, COS will have a set of bright limit restrictions that may preclude some objects from being observed. Since the throughput of COS is considerably higher than that of STIS, it may be necessary to observe some bright sources with STIS rather than COS, or else use the bright object aperture with COS (see Section 2.3).

COS has two general types of bright limits: global and local. At FUV wavelengths, the ACCUM mode global bright limit is ~60,000 cnt s^{-1} $segment^{-1}$, and the local count rate limit is ~1.67 cnt s^{-1} pix^{-1} (~100 cnt s^{-1} $resel^{-1}$). At NUV wavelengths, the ACCUM mode global bright limit is ~170,000 cnt s^{-1}, and the local count rate limit is ~200 cnt s^{-1} pix^{-1} (~1800 cnt s^{-1} $resel^{-1}$). The NUV ACCUM mode global count rate limit can be

increased slightly at the expense of Doppler compensation during the course of the exposure.

Figure 5: COS FUV point source sensitivities.

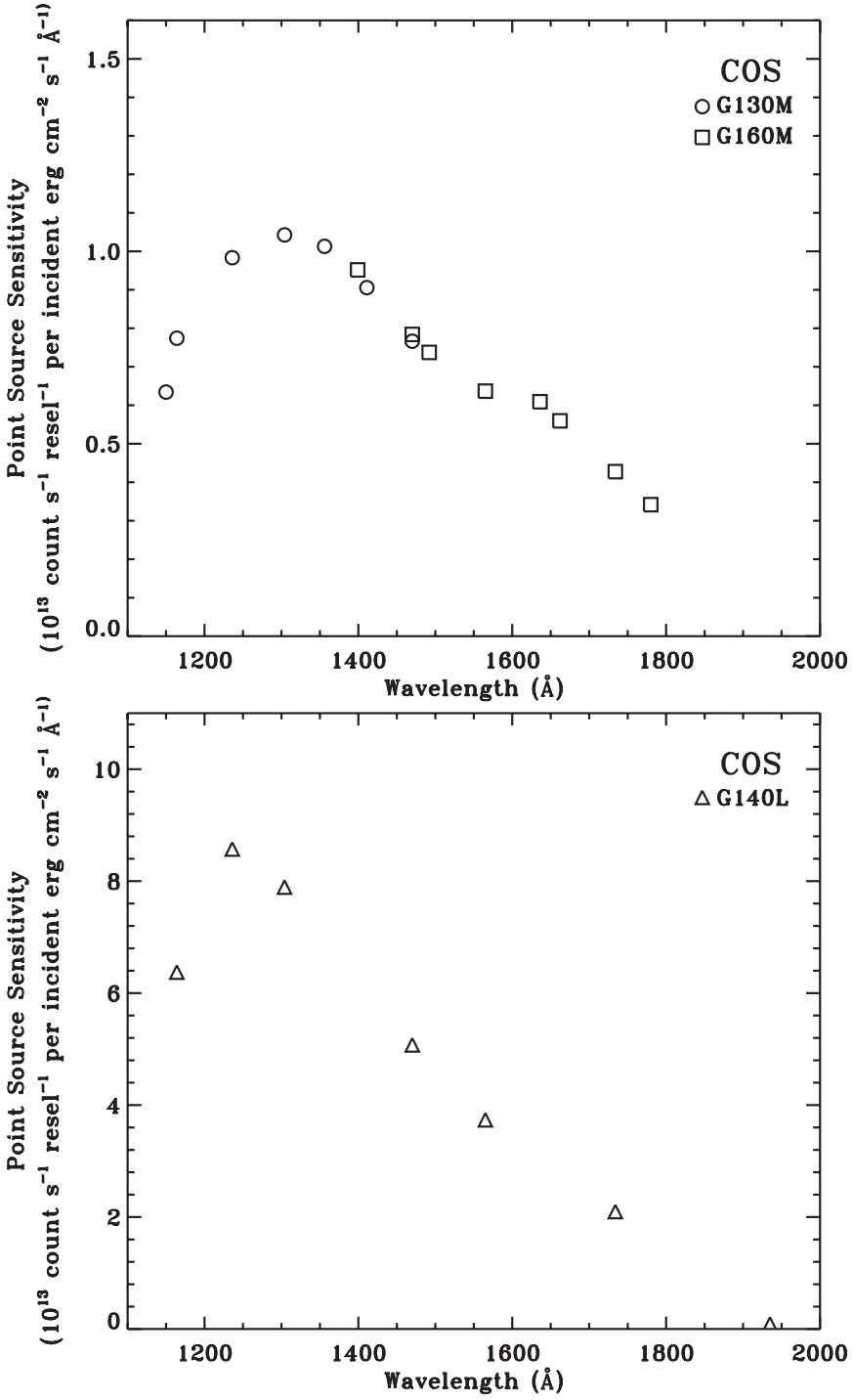

Figure 6: COS NUV point source sensitivities.

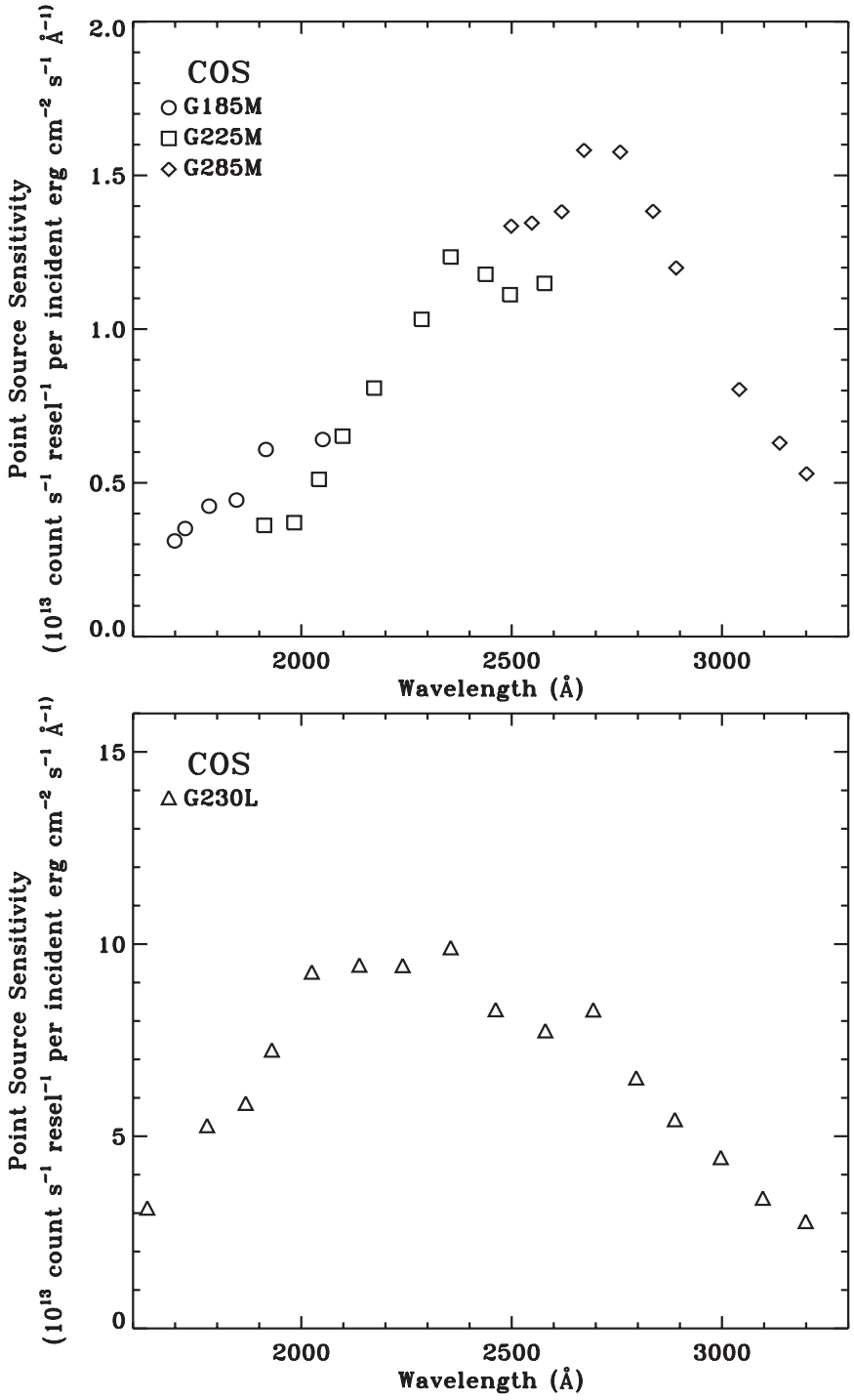

Table 5: COS/STIS Sensitivity Comparison

Mode	λ/Δλ	Binning	S_λ (10^{13} cnt s^{-1} $resel^{-1}$) / (erg cm^{-2} s^{-1} $Å^{-1}$)		
FUV Modes			**λ = 1300 Å**	**λ = 1600 Å**	
COS G130M COS G160M	20,000	---	1.0	0.69	
	10,000	x2	2.0	1.4	
	2,500	x8	8.0	5.5	
	1,000	x20	20.	14.	
STIS E140M	45,800	---	0.060	0.024	
	20,000	x2.3	0.14	0.055	
STIS G140M	10,000	---	0.66	0.13	
	2,500	x4	2.6	0.52	
COS G140L	2500	---	7.9	3.4	
	1,000	x2.5	20.	8.5	
STIS G140L	1,000	---	12.6	3.0	
NUV Modes			**λ = 1800 Å**	**λ = 2300 Å**	**λ = 2800 Å**
COS G185M COS G225M COS G285M	20,000	---	0.43	1.1	1.5
	10,000	x2	0.86	2.2	2.0
	2,500	x8	3.4	8.8	12.
	500	x40	17.	44.	60.
STIS E230M	30,000	---	0.062	0.30	0.36
	20,000	x1.5	0.093	0.45	0.54
STIS G230M	10,000	---	0.20	0.94	1.0
	2,500	x4	0.80	3.8	4.1
COS G230L	2,500	---	5.2	9.4	6.5
	500	x5	26.	47.	32.
STIS G230L	500	---	8.8	32.	34.

Note: Backgrounds are not included in the listed sensitivities. In background-limited situations, the expected S/N calculated from these numbers must include background information, and comparisons of different instrument modes will depend upon the details of the background and the spectral bin size adopted. Values for all STIS modes assume 2 pixels per resolution element and no slit transmission losses. Use of the 0.2" x 0.2" aperture reduces the STIS values by factors of 1.3 (2800 Å) to 1.8 (1300 Å). Use of the 0.2" x 0.06" slit reduces the STIS values by factors of 1.7 (2800 Å) to 2.6 (1300 Å). The STIS echelle values do not account for scattered light, which is a substantial component of the background (especially for E140M); including echelle scattered light will further reduce the STIS values of S_λ.

Table 6 contains approximate estimates of the bright limit fluxes for the medium- and low-resolution COS modes at several wavelengths using the count rate limits listed in Table 2. Below each flux limit we also list the approximate corresponding visual magnitude of an unreddened O9 V star. The final operational screening limits set by STScI may be more restrictive than those listed in Table 6.

Users should note that the minimum exposure time allowed for COS exposures is 0.1 second. Exposures shorter than a few minutes will be dominated by overheads associated with setting up the exposure and obtaining wavelength calibration exposures. The maximum exposure time allowed for a single exposure (or FP-split sub-exposure) is 6500 seconds.

Table 6: COS Bright Limits

λ Region	λ (Å)	Local Limit (erg cm^{-2} s^{-1} Å^{-1}) [V mag of O9 V star]		Global Limit (Flat spectrum: erg cm^{-2} s^{-1}Å^{-1}) [V mag of O9 V star]	
		R ~ 20,000 (M gratings)	R ~ 2,500 (L gratings)	R ~ 20,000 (M gratings)	R ~ 2,500 (L gratings)
FUV	1300	9.6×10^{-12} [~11.3]	1.3×10^{-12} [~13.5]	1.9×10^{-12} [~13.0]	7.8×10^{-13} [~ 13.7]
	1600	1.6×10^{-11} [~10.1]	3.1×10^{-12} [~11.9]	1.9×10^{-12} [~12.3]	
NUV	1800	4.2×10^{-10} [~6.3]	3.4×10^{-11} [~9.0]	2.6×10^{-11} [~9.0]	6.8×10^{-12} [~11.4]
	2300	1.7×10^{-10} [~9.0]	1.9×10^{-11} [~11.4]	2.4×10^{-11} [~10.3]	
	2800	1.2×10^{-10} [~6.2]	2.8×10^{-11} [~7.7]	2.0×10^{-11} [~6.8]	

Note: Bright limits are for point sources centered in the PSA. These numbers increase by a factor of ~100 [5 magnitudes] if the BOA is used. Global limits assume either a flat spectrum or an unreddened O9 V stellar spectrum observed in ACCUM mode. For the medium-resolution modes, the global limits are appropriate for a spectral region centered roughly on the specified wavelength. For the low-resolution modes, the global limits are appropriate for grating tilts with central wavelengths of 1230 Å and 2635 Å. Screening limits adopted for nominal operations may be more restrictive than those listed in this table.

3.4 Backgrounds

For faint sources, backgrounds can be a significant source of counts detected by COS and must be considered when making exposure time estimates if flux levels are less than ~10^{-15} erg cm^{-2} s^{-1} $Å^{-1}$. The background events arise mainly from radioactive decays in the materials used to construct the microchannel plates and associated hardware. For the windowless FUV MCP detector, the on-orbit background rate is expected to be similar to the rate of ~0.5-0.8 cnt s^{-1} cm^{-2} (~7.5×10^{-7} cnt s^{-1} pix^{-1}) measured for the FUSE MCP detectors. However, like the STIS NUV MAMA, the COS NUV MAMA suffers significantly increased background levels due to fluorescence caused by impurities in its MgF_2 window. The expected on-orbit background level is ~34 cnt s^{-1} cm^{-2} (~2.1×10^{-4} cnt s^{-1} pix^{-1}), which is about a factor of 4 lower than the background level found for the STIS flight MAMA (Ball SER COS-NUV-001). Low energy thermal ions are excluded from the COS detectors through the use of ion repeller grids. Scattered light is not expected to be a significant source of background on either COS detector since the COS first-order diffraction grating rulings have very low scatter (<2×10^{-5} / Å). Full characterization of the intrinsic pre-flight backgrounds and on-orbit backgrounds for both COS detectors will be performed to assess the impact of the detector and scattered light backgrounds on observations of faint objects.

4. Choosing Between COS and STIS

4.1 General Considerations

The spectral resolution, wavelength coverage, and sensitivity required for an observation will often be the most important factors involved in deciding whether to use COS or STIS for an ultraviolet spectroscopic observation of a point source. Spectral resolutions and wavelength coverages available for each instrument are summarized above in Tables 3 and 4. Sensitivities are compared in Table 5.

Wavelength ranges for selected COS and STIS spectroscopic modes are shown in Figure 7. Note that multiple wavelength settings may be required in some modes to cover the entire NUV channel (e.g., COS and STIS M gratings). Observing programs needing full wavelength coverage may benefit from observations made with lower sensitivity or lower resolution modes requiring fewer exposures to cover the entire wavelength range.

COS has limited scientific imaging capabilities in the 1700–3200 Å bandpass. The field of view is limited to the aperture size of 2.5 arcsec, which may be sufficient for point source target confirmation. Most observing programs that require two-dimensional imaging at ultraviolet wavelengths should use another HST instrument, such as ACS, STIS, or WFC3.

Figure 7: Wavelength coverages available with common COS and STIS spectroscopic modes. Ranges for different grating tilts are offset in the vertical direction. Additional settings may be available for some modes.

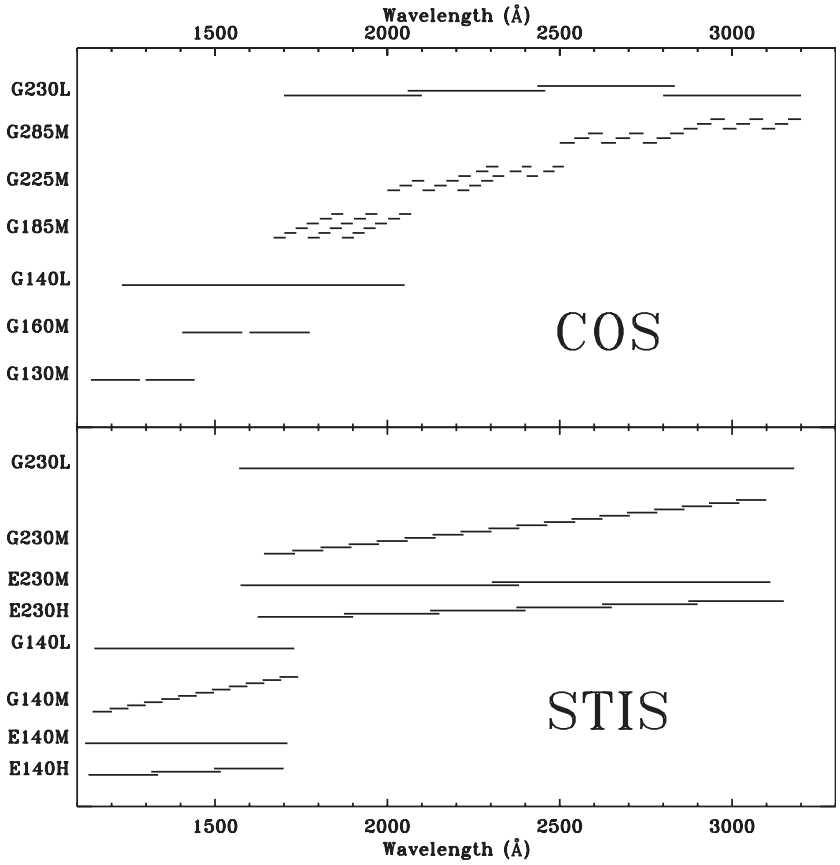

4.2 Recommended Choices

In Table 7 we list some typical types of spectroscopic observations and recommendations as to whether observers should use COS or STIS for their observations. These are general guidelines only, with the ultimate choice of instrument left as a decision to the proposer.

Table 7: Which Instrument Is Right For Your Observation – COS or STIS?

Type of Observation	Recommended Instrument	Comments
High resolution FUV/NUV spectroscopy (point source)	STIS	R ~ 100,000 (echelle modes) R ~ 200,000 (narrowest slit)
Medium resolution FUV/NUV spectroscopy (point source)	COS	R ~ 20,000, high throughput, but less λ coverage than STIS echelle
Low resolution FUV/NUV spectroscopy (faint point source, above background limit)	COS	R ~ 2500, high throughput, low background, large λ coverage
Low resolution FUV/NUV spectroscopy (faint point source, background-limited)	COS/STIS	Choice depends on details of background and wavelength
Low resolution FUV/NUV spectroscopy (bright point source)	COS	R ~ 20,000 binned to produce very high throughput
Optical spectroscopy ($\lambda > 3200$ Å)	STIS	N/A with COS
Longslit spectroscopy of extended sources	STIS	N/A with COS
Slitless spectroscopy of extended sources	STIS	N/A with COS
FUV/NUV spectroscopy of very bright objects	COS / STIS	May be too bright for COS, choice depends on resolution
Rapid UV variability, timing information required	COS / STIS	TTAG mode; use STIS if $\Delta t < 32$ ms is required
Crowded-field FUV spectroscopy (<1 arcsec confusion limit)	STIS	COS may be acceptable if confusion limit is >1 arcsec

5. Target Acquisitions

COS will have several target acquisition procedures designed for accurate positioning of astronomical sources in the science apertures. These procedures will include standard target searches, dispersed light peak-ups, autonomous NUV imaging acquisitions, and offset acquisitions. All target acquisitions will occur using light at ultraviolet (not optical) wavelengths; the exact wavelength will depend upon the acquisition mode chosen. The algorithms for these procedures will be optimized for point sources, but extended source acquisitions should be possible as well. Typical imaging target acquisition sequences are expected to require approximately 5 minutes. Times for dispersed light acquisitions will depend on source flux levels. Details about these procedures will be given in the full COS Instrument Handbook released with the Cycle 13 Call for Proposals.